Applied Chemical Engineering (2021) Volume 4 Issue 2
doi:10.24294/ace.v4i2.1351

ORIGINAL RESEARCH ARTICLE

Synthesis of carbon-based CoV electrocatalyst and its application in Zn-air battery devices

Zhuo Li, Fangling Zhou, Lei Wang*, Honggang Fu*

Key Laboratory of Functional Inorganic Material Chemistry, School of Chemistry and Materials Science, Heilongjiang University, Harbin 150080, China. E-mail: wanglei0525@hlju.edu.cn; fuhg@hlju.edu.cn

ABSTRACT

Precious metal catalysts are generally considered to be the best electrocatalysts for slow four-electron transfer mechanism in oxygen reduction and oxygen evolution reactions. However, its large-scale commercialization is limited due to its high cost, scarce resources and lack of stability. Therefore, under the same catalytic performance conditions, low cost and environmentally friendly non-noble metal electrocatalyst will become the focus of future electrocatalyst engineering. Dicyandiamine was used for carbon resource to prepare CoV-based carbon nanotube composites (named CoV-NC) by means of group coordination combined with freeze drying strategy and carbonization treatment. The morphology and structure of the sample was characterized by scanning electron microscopy (SEM), X-ray diffraction (XRD) and N_2 adsorption-desorption curve. In 0.1 M KOH electrolyte, the E_{onset} potential of CoV-NC catalyst for ORR is 0.931 V, and the limiting current density is higher. The OER voltage is only 1.63 V at the current density of 10 mA·cm^{-2}, demonstrating that CoV-NC exhibits good catalytic activity of ORR and OER. As for an air-cathode material to assemble primary Zn-air battery, it can discharge continuously for 166 h at a current density of 5 mA·cm^{-2}, which is much better than commercial Pt/C catalyst.

Keywords: Nitrogen-doped Carbon; Transition Metal; Electrocatalyst; Oxygen Reduction Reaction; Zn-air Battery

ARTICLE INFO

Received: 5 July 2021
Accepted: 17 August 2021
Available online: 22 August 2021

1. Introduction

With the continuous development and improvement of human social productivity, people's demand for energy is increasing. Finding, developing and utilizing sustainable renewable energy is the focus of human scientific research[1–3]. Zn-air battery is one of the main categories in metal air battery at present. Compared with other metal air battery products, Zn-air battery has good business prospects because of its high reliability, high specific energy, stable charge and discharge characteristics, small self-discharge, low price, environmental friendliness, long service life and good reversibility[4–8]. Noble metal Pt-based catalyst has long been considered as the best electrocatalyst for ORR slow four electron transfer mechanism. However, due to its high price and scarce resources, it not only increases the cost, but also is not conducive to large-scale commercial production[9–12]. Therefore, the main research focuses on non-metallic catalysts, and it is found that the catalytic performance and stability of N-doped catalysts in carbon materials are more effective than Pt/C-based catalysts. It was found that hybrid catalysts doped with transition metal (e.g. Fe and Co) nanoparticles in

N-doped carbon materials showed better activity for ORR[12–16].

Using dicyanodiamine as nitrogen-containing carbon source, Co and V metal species were introduced based on group coordination. The precursor was obtained by freeze-drying method, and then CoV-NC carbon nanotubes were obtained by high temperature calcination. Then the samples were characterized by SEM and XRD. Finally, their oxygen reduction performance was tested and applied to the study of Zn-air battery. By testing, it is found that the prepared CoV-NC catalyst has excellent ORR and OER catalytic properties. At the same time, the Zn-air battery assembled with this material as the cathode material also has a long discharge time and shows good application value.

2. Experiment

2.1 Instruments and reagents

Instruments: CHI660 electrochemical workstation (Shanghai CH Instruments Co., Ltd.); Bruker D8 X-ray diffractometer (Bruker, Germany); Hitachi S-4800 scanning electron microscope (Hitachi, Japan).

Reagents: dicyanodiamine (AR), ammonium metavanadate (AR), cobalt chloride hexahydrate (AR), Nafion (5%), ethanol (AR), potassium hydroxide (AR).

2.2 Experimental method

2.2.1 Material synthesis

Add 2.102 g of dicyanodiamine into 50 mL of water in a 100 mL beaker to dissolve it. The dissolution temperature is 38 °C, and stir fully. Dissolve 0.2379 g cobalt chloride hexahydrate and 0.5 mmol ammonium metavanadate in 10 mL water at 50 °C and stir fully. Slowly drop the sample into the dissolved dicyanodiamine solution and stir for 1 h. The sample solution is orange red. Freeze dry the stirred sample to obtain the sample precursor, then put it in a porcelain boat, place it in a high-temperature tubular furnace, carbonize it under nitrogen atmosphere of 800 °C for 2 h, and set the heating rate as 5 °C·min^{-1}. After high temperature calcination, the sample is CoV-NC carbon nanotube, named CoV-NC-800 (800 °C). For comparison, samples at different carbonization temperatures were prepared, named CoV-NC-700 (700 °C) and CoV-NC-900 (900 °C).

Using the same preparation method, only 0.2379 g cobalt chloride hexahydrate was added to obtain Co-NC carbon nanotubes, named Co-NC; similarly, only 0.5 mmol ammonium metavanadate was added to obtain V-NC carbon nanotubes, named V-NC.

2.2.2 Electrochemical performance test

The electrochemical test adopts a three-electrode system: glassy carbon ring disk electrode as the working electrode, commercial reversible hydrogen electrode as the reference electrode and platinum electrode as the counter electrode. The diameter of glassy carbon rotating ring disk electrode is 5.61 mm. Before the modification of the working electrode, it was polished with 50 nm Al_2O_3, ultrasonic cleaned repeatedly with ethanol and ultrapure water, and finally the electrode surface was dried with N_2. The working electrode was modified: 5 mg catalyst was mixed with 1.5 mL ethanol and 0.5 mL Nafion (0.5 wt%) and sonicated for 30 mins to obtain uniform catalyst dispersion. Then, the dispersion was coated on the surface of the glassy carbon electrode and dried under an infrared lamp with a catalyst loading of 0.4 mg·cm^{-2}. In order to compare the electrochemical performance of the catalyst, the commercial Pt/C (20 wt%) catalyst dispersion was prepared by the same method.

Cyclic voltammetry (CV) and linear sweep voltammetry (LSV) were measured at 0–1.2 V potential and O_2 saturated 0.1 M KOH. The LSV of the catalyst was measured by rotating disk electrode (RDE) with scanning rate of 5 mV·s^{-1} at different rotating speeds (400–2,500 r·min^{-1}). The electron transfer number n in ORR process is calculated by Koutecky-Levich (K-L) equation:

$$1/J = 1/J_L + 1/J_K = 1/(B\omega^{1/2}) + 1/J_K \qquad (1)$$

$$B = 0.62nFC_0D_0^{2/3}V^{1/6} \qquad (2)$$

The yield of n and hydrogen peroxide in ORR process (H_2O_2 (%)) was calculated using LSV experimental data:

$$H_2O_2(\%) = 200 \times \frac{I_r/N}{I_d + I_r/N} \tag{3}$$

$$n = 4 \times \frac{I_d}{I_d + I_r/N} \tag{4}$$

In the equation, I_r is ring current; I_d is disk current; N is the collection coefficient of the rotating ring disk electrode, and its value is 0.37.

The preparation of OER working electrode is the same as that of ORR working electrode. The potential is 1–2 V and the scanning speed is 5 $mV \cdot s^{-1}$.

2.2.3 Performance test of Zn-air battery

The self-made Zn-air battery was used for battery performance test: 2 cm × 2 cm self-supporting carbon nanofiber film was directly used as air cathode, and the polished 3 cm × 7 cm zinc sheet as anode and 6 M KOH solution containing 0.2 M $Zn(CH_3COOH)_2$ as electrolyte Zn-air battery. The power density, primary discharge and open circuit voltage of the battery are tested by Land-CT2001A system.

3. Results and discussion

3.1 Material composition and structural characterization

The comparative spectra of CoV-NC-800, Co-NC and V-NC scanning electron microscope (SEM) are shown in **Figure 1**. As can be seen from **Figure 1(a)**, CoV-NC-800 carbon nanotubes are relatively uniform; as can be seen from **Figure 1(b)**, the size of CoV-NC-800 carbon nanotube is about d = 100 nm, in the shape of bamboo; it can be seen from **Figure 1(c)** and **Figure 1(d)** of the comparison sample that Co-NC and V-NC are mainly in block structure with uneven size.

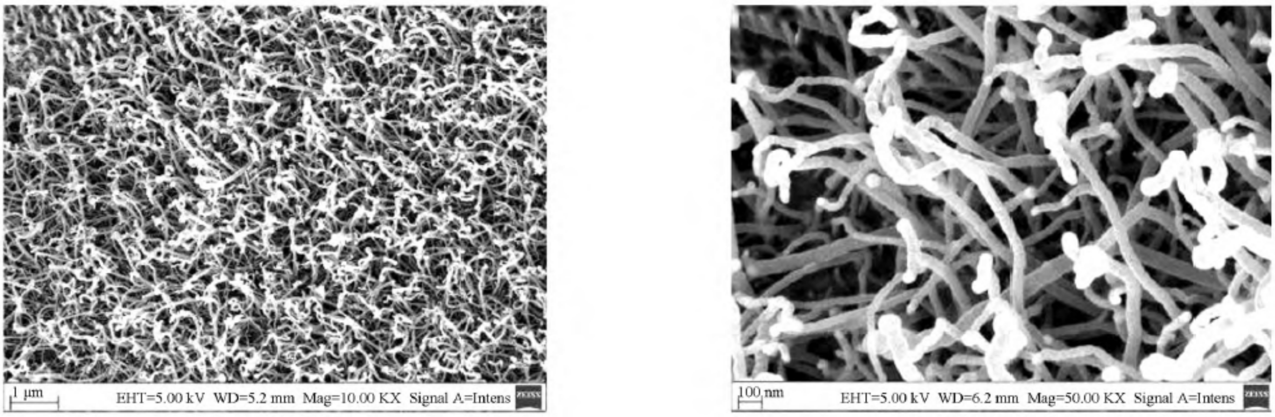

(a) CoV-NC-800 (b) CoV-NC-800

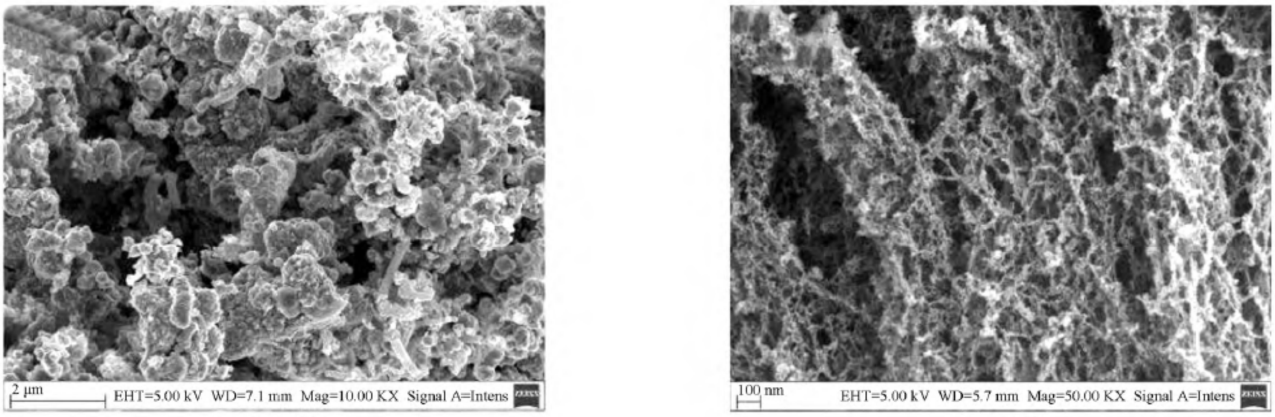

(c) Co-NC (d) V-NC

Figure 1. SEM spectrum.

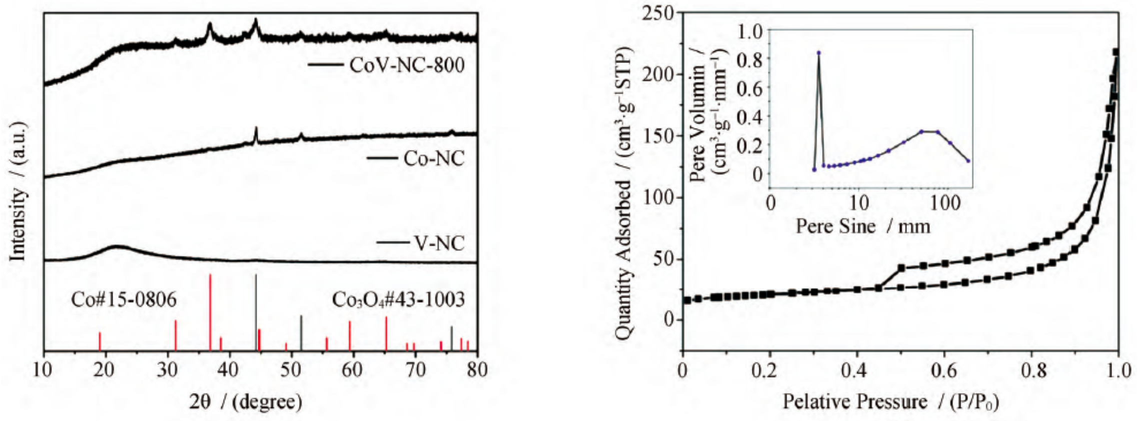

(a) (b)

Figure 2. (a) XRD pattern of CoV catalysts and standard patterns of Co and Co_3O_4; **(b)** N_2 isotherm adsorption-desorption curve.

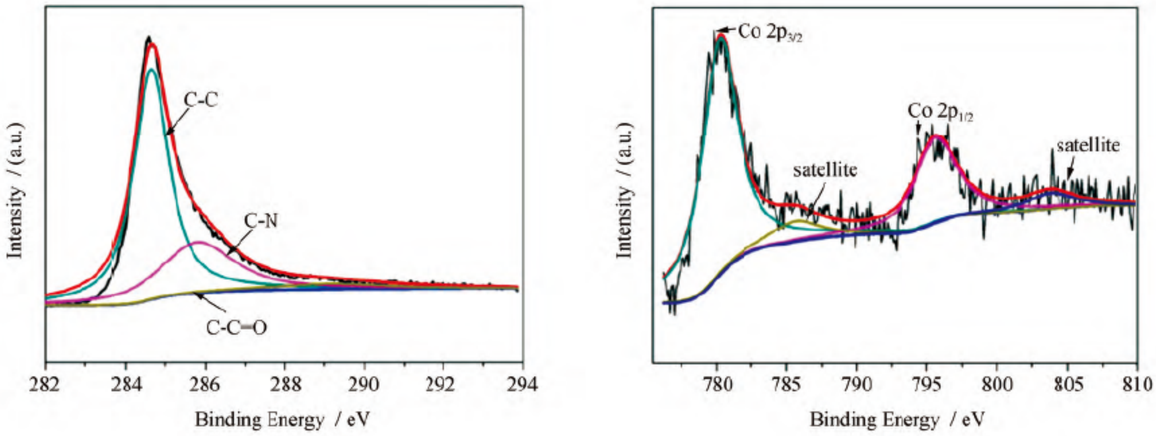

(a) C 1s (b) Co 2p

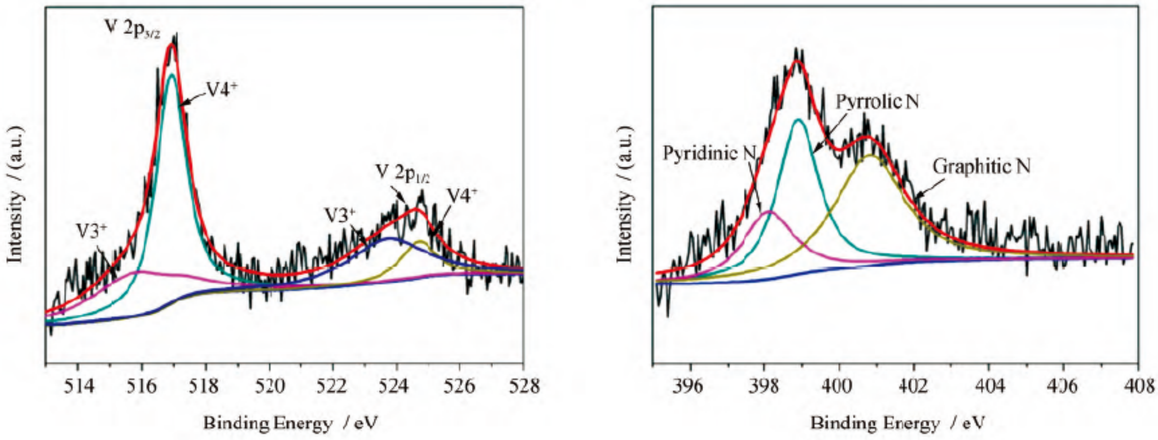

(c) V 2p (d) N 1s

Figure 3. High-resolution XPS spectra.

The composition of the material was characterized by XRD, as shown in **Figure 2(a)**. As can be seen from **Figure 2(a)**, the XRD spectrum of Co-NC catalyst presents strong diffraction peaks when $2\theta = 44.2°$, 51.5° and 75.9°, and three obvious peaks correspond to (111), (200) and (220) crystal planes of metal Co, respectively. The V-NC sample has a wide diffraction peak at 20°–30°, indicating that the sample contains amorphous carbon. No peak related to V species was detected in the sample, which may be due to the low content of V. The XRD pattern of CoV-NC catalyst shows the peaks of Co and Co_3O_4, indicating that the addition of V helps to convert part of Co into Co_3O_4. In order to further determine the micro pore structure of the material, N_2 adsorption desorption measurement was carried out on the sample, as shown in **Figure 2(b)**. As can be seen from **Figure 2(b)**, the adsorption isotherms of all samples are type IV curves with obvious hysteresis rings, indicating that there are a large number of mesoporous structures, which corresponds to the SEM diagram. In addition, the specific surface area of CoV-NC is 68.3732 $m^2 \cdot g^{-1}$, which is conducive to the contact between O_2 and active sites and improve the mass transfer rate.

3.2 XPS characterization of materials

X-ray photoelectron spectroscopy (XPS) (**Figure 3**) can not only determine the composition of surface elements, but also give the chemical and electronic state information of each element. As can be seen from **Figure 3(a)**, there are three peaks in the C 1s spectrum, namely C-C (284.6 eV), C-N (285.8 eV) and C-C=O (289.1 eV). The existence of CN bond and the obvious asymmetry of C 1s peak prove the heteroatom doping in graphite carbon network. As can be seen from **Figure 3(b)**, there are two peaks in the Co 2p spectrum, namely Co $2p_{3/2}$ (780.2 eV) and Co $2p_{1/2}$ (795.6 eV). As can be seen from **Figure 3(c)**, there are four peaks in V 2p spectrum, and the contents of V^{3+} and V^{4+} are 515.8/516.9 and 523.7/524.7 eV, respectively. As can be seen from **Figure 3(d)**, the high resolution N 1s spectrum can be divided into three peaks located at 398.1, 399.0 and 400.8 eV, which are attributed to pyridine N, pyrrole N and graphite N, respectively.

3.3 Electrocatalytic ORR and OER properties of materials

The LSV of the catalyst was measured by rotating disk electrode (RDE) and rotating ring disk electrode (RRDE) in O_2 saturated 0.1 mol·L^{-1} KOH solution at 1,600 r·min^{-1}. The initial potential (E_{onset}) of the catalyst was 0.931 V. The ORR polarization curves of CoV-NC catalyst at different calcination temperatures are compared, as shown in **Figure 4**. It can be seen from **Figure 4** that the half wave potential ($E_{1/2}$) of 800 °C CoV-NC is 0.834 V, which is higher than 700 °C (0.829) and 900 °C (0.794). It shows that the ORR performance of CoV-NC is the best at 800 °C. The ORR and OER polarization curves of CoV-NC-800 and different comparison samples are shown in **Figure 5** and **Figure 6**, respectively. It can be seen from **Figure 5** that at 800 °C, CoV-NC shows ORR activity equivalent to Pt/C catalyst, and the half wave potential ($E_{1/2}$) is 0.834 V, which is higher than Co-NC (0.768 V) and V-NC (0.826 V), confirming the excellent ORR activity of Co-NC. It can be seen from **Figure 6** that CoV-NC shows excellent OER catalytic performance at 800 °C. At 10 mA·cm^{-2}, the potential of CoV-NC is 1.63 V, which is lower than that of Co-NC (1.74 V) and V-NC (1.75 V), which proves the excellent OER activity of Co-NC.

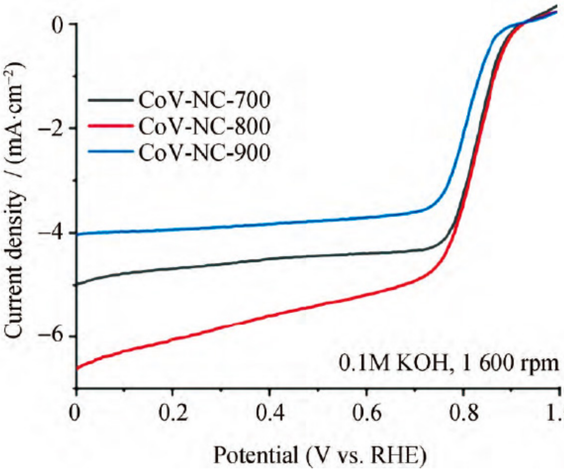

Figure 4. ORR polarization curves of CoV-NC catalyst at different calcination temperatures.

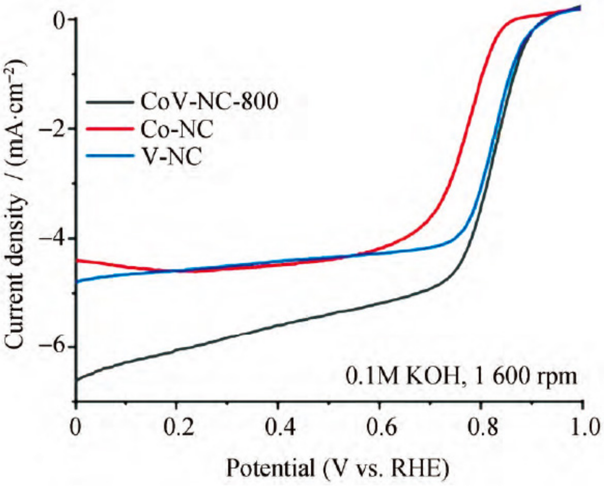

Figure 5. ORR polarization curves of CoV-NC-800 catalyst at different calcination temperatures.

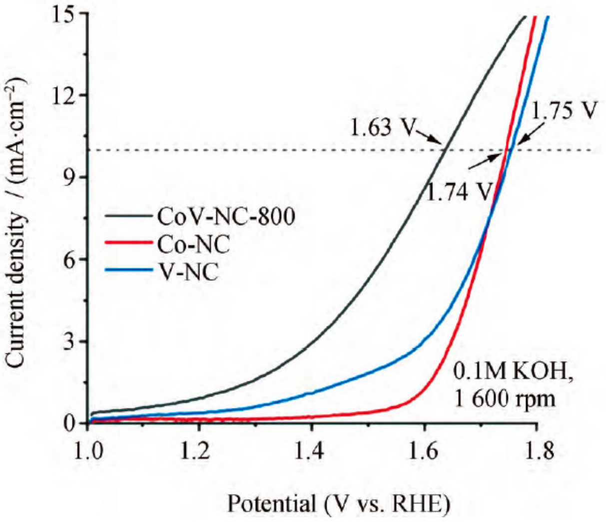

Figure 6. ORR polarization curves of CoV-NC-800 at different comparison samples.

3.4 Performance test of Zn-air battery

In order to test the application effect of the prepared catalyst in practice, it was used as a self-supporting air cathode to assemble Zn-air air battery, and a series of performance tests were carried out. The constant current discharge curve is shown in **Figure 7**. It can be seen from **Figure 7** that the primary Zn-air battery assembled with CoV-NC-800 as positive material can discharge continuously for 166 h at 5 mA·cm^{-2}, which is longer than that of Pt/C.

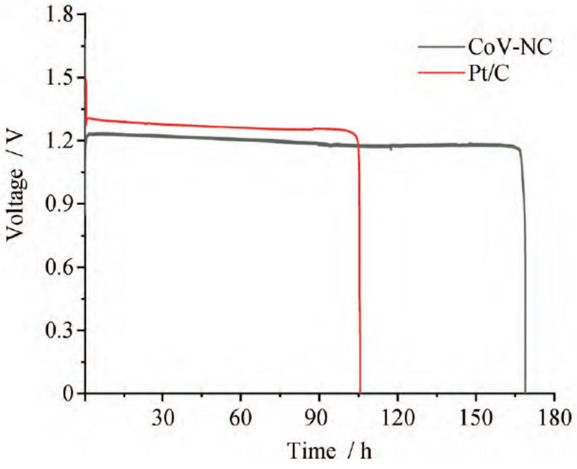

Figure 7. Discharge test of N-air battery under current density of 5 mA·cm^{-2}.

4. Conclusion

Using dicyanodiamine as nitrogen-containing carbon source, the catalyst precursor was obtained by low-temperature freeze-drying, and then CoV-NC carbon nanotubes were obtained by high-temperature calcination. Different catalysts CoV-NC were prepared by changing the carbonization reaction temperature. Finally, the samples were tested for ORR electrochemical performance in alkaline system, to determine the initial potential, half wave potential and limit current density of ORR reaction. After testing, it is found that the prepared CoV-NC has high initial potential and high limit current density. Compared with the general reversible hydrogen electrode, its initial potential can reach 0.931 V, the limit current density is very large, and the voltage of CoV-NC catalyst at 10 mA·cm^{-2} is 1.63 V, the potential is lower than that of single metal catalyst. It is proved that CoV-NC has good ORR and OER catalytic activities. The primary Zn-air battery assembled by CoV-NC as positive material can discharge continuously for 166 h at 5 mA·cm^{-2}, which is better than commercial Pt/C catalyst, and has a broad application space in the field of energy devices.

Conflict of interest

The authors declare that they have no conflict of interest.

Acknowledgements

General Project of National Natural Science Foundation of China (21771059); Heilongjiang Excellent Youth Fund Project (YQ2019B007).

References

1. Ma L, Chen S, Wang D, *et al.* Super-stretchable zinc-air batteries based on an alkaline-tolerant dual-network hydrogel electrolyte. Advanced Energy Materials 2019; 9: 1803046.
2. Chen X, Zhou Z, Karahan HE, *et al.* Recent advances in materials and design of electrochemically rechargeable zinc-air batteries. Small 2018; 8: 1–29.
3. Stacy J, Regmi YN, Leonard B, *et al.* The recent progress and future of oxygen reduction reaction catalysis: A review. Renewable and Sustainable Energy

Reviews 2017; 69(6): 401–414.

4. Cui SH, Sun LP, Kong FH, *et al.* Carbon-coated $MnCo_2O_4$ nanowire as bifunctional oxygen catalysts for rechargeable Zn-air batteries. Power Sources 2019; 8: 25–31.
5. Li M, Luo F, Zhang Q, *et al.* Rational construction of self-standing sulfur-doped Fe_2O_3 anodes with promoted energy storage capability for wearable aqueous rechargeable NiCo-Fe batteries. Advanced Energy Materials 2020; 7: 2001064.
6. Naoya A, Hideo I, Akira S, *et al.* Electrochemical and chemical treatment methods for enhancement of oxygen reduction reaction activity of Pt shell-Pd core structured catalyst. Electrochimica Acta 2017; 8: 146–153.
7. Yu L, Yu X, Luo XW. The design and synthesis of hollow micro-/nanostructures: Present and future trends. Advanced Materials 2018; 30(38): 1800939.
8. Li Z, Li M, Bian Z, *et al.* Design of highly stable and selective core/yolk–shell nanocatalysts — A review. Applied Catalysis B: Environmental 2016; 188: 324–341.
9. Burke MS, Enman LJ, Batchellor AS, *et al.* Oxygen evolution reaction electrocatalysis on transition metal oxides and (oxy) hydroxides: Activity trends and design principles. Chemistry of Materials 2015; 27(22): 7549–7558.
10. Chitturi VR, Ara M, Fawaz W. Enhanced lithium-oxygen battery performances with Pt subnanocluster decorated N-doped single-walled carbon nanotube cathodes. ACS Catalysis 2016; 6(10): 7088–7097.
11. Nørskov JK, Rossmeisl J, Logadottir A, *et al.* Origin of the overpotential for oxygen reduction at a fuel-cell cathode. The Journal of Physical Chemistry B 2004; 108(46): 17886–17892.
12. Liang J, Jiao Y, Jaroniec M, *et al.* Sulfur and nitrogen dual-doped mesoporous graphene electrocatalyst for oxygen reduction with synergistically enhanced performance. Angewandte Chemie International Edition 2012; 5: 11496–11500.
13. Li M, Xiong N, Zhou X*, et al*. Controllable fabrication of Fe_3S_4 nanocrystals and electrocatalytic hydrogen evolution properties. Journal of Engineering of Heilongjiang University 2020; 11(1): 41–47.
14. Zheng X, Wu J, Cao X, *et al.* N-, P-, and S-doped graphene-like carbon catalysts derived from onium salts with enhanced oxygen chemisorption for Zn-air battery cathodes. Applied Catalysis B: Environmental 2019; 241: 442–451.
15. Wang Z, Li B, Ge X, *et al.* $Co@Co_3O_4@PPD$ core@bishell nanoparticle-based composite as an efficient electrocatalyst for oxygen reduction reaction. Small 2016; 12(19): 2580–2587.
16. Gu P, Zheng M, Zhao Q, *et al.* Rechargeable zinc-air batteries: A promising way to green energy. Journal of Materials Chemistry A 2017; 5(17): 7651–7666.